35th EPS Conference on Plasma Phys. Hersonissos, 9 - 13 June 2008 ECA Vol.**32D**, P-2.015 (2008)

Quasineutral kinetic simulation of the scrape-off layer: Asymmetric ELM energy deposition on divertor plates

James P. Gunn,[1] Vladimir Fuchs[2]

[1] *Association EURATOM-CEA, 13108 St Paul Lez Durance, France.*

[2] *Association EURATOM-IPP.CR , PO Box 17, 18 200 Praha 8, Czech Republic*

Following the collapse of the tokamak H-mode pedestal and the formation of an edge-localized mode (ELM), plasma particles and power are transported along field lines to the divertor targets[1]. Salient features of ELM energy deposition on divertor targets have been reproduced by a simple collisionless free-streaming ion model[2]. The temporal evolution of power flux onto a divertor plate repoduces reasonably well measurements by infrared cameras. The peak power flux arrives first on the outboard plate, then the inboard plate. The delay is independent of the B-field direction. This can be explained by the observation that the ELM plasma enters the SOL on the outboard side of the torus; the delay is simply caused by the difference in connection lengths between the outboard midplane and each target plate. The ratio of ELM energy deposition onto inner and outer plates is asymmetric. With $\boldsymbol{B}\times\nabla\boldsymbol{B}$ directed towards the X-point, $E_{in}E_{out}$~2 is typically observed. The asymmetry reverses when $\boldsymbol{B}$ is reversed. It was recently proposed that the asymmetry could be due to EXB rotation of the ELM filaments in the edge region where the radial electric field is directed inwards[3]. Including a net fluid drift in the simple model, it is found that ELM Mach numbers of the order of 0.2 (evaluated using pedestal plasma parameters) can reproduce the asymmetry.

Ion and electron velocity distributions in the ELMy SOL may depart significantly from thermal conditions in low or intermediate collisionality regimes. The transient nature of an ELM event can lead to rapidly evolving non-thermal distributions that can only be modelled correctly by a kinetic approach. The ELM problem has been investigated using a particle-in-cell (PIC) code[4]. Classical PIC methods obtain the electric field from Poisson's equation and are thereby restricted to resolving the Debye scale. In order to obtain solutions, the real length scale of the problem (10s of m along field lines) must be drastically reduced (to the order of cm), and still, the CPU run time can reach days or weeks.

We apply a novel particle simulation technique[5] to the 1D SOL problem. Rather than solving Poisson's equation, the quasineutral particle-in-cell (QPIC) approach uses the electron fluid momentum equation to calculate the electric field. QPIC can simulate time and spatial scales much larger than the plasma period and Debye length. For example, a realistic SOL can be simulated with cell size of 1 m and a time step proportional to the electron transit time across a cell. The steady state kinetic solution can be obtained with reasonable resolution in a few minutes on a personal computer. The code has been benchmarked[6] against the kinetic solution of the Mach probe problem[7]. In this contribution we will show new results for a bounded 1D SOL into which we introduce an ELM pulse. The target boundary conditions include self-consistent sheath potentials allowing electric current circulation between the targets[8].

Each ELM is injected into a stationary thermal SOL solution provided by QPIC. To get this solution, we approximate radial transport from the confined plasma (characterized by separatrix plasma parameters) as a volumetric source term in the 1D Vlasov equation. The SOL is divided into 50 cells along the parallel direction. Each cell would contain 10000 ions or electrons if its density were equal to the separatrix density (the real local density is of course much lower due to parallel losses). Then, the ELM is simulated as the sudden appearance of dense, hot plasma in a thin region at the center of the simulation domain. We choose the parallel length of the initial ELM filament to be 0.2 of the total connection length. The ELM density and temperature are given by mid-pedestal plasma parameters, which we take to be 4 times those at the separatrix. Both ions and electrons are assigned Maxwellian distributions shifted by the same constant velocity. An ion-to-electron mass ratio of 1836 was used. The simulation runs for a few ion transit times until the ELM perturbation completely disappears and the thermal SOL solution is recovered. During the run all the fluid moments at each target are recorded, as well as the sheath floating potentials and net parallel current through the SOL.

Power and particle fluxes for ELM Mach number M_{ELM}=0.35 are shown in Fig. 1 and Fig. 2 respectively. An initial heat pulse due to hot electrons is observed after a delay Δt_e given by the time of flight from the midpoint of the simulation region. The delay as well as the magnitude of the electron power flux is the same at both targets and independent of the ELM Mach number, because $M_{\mathrm{ELM}} \ll v_{\mathrm{Te,ped}}$. Despite significant electron power flow, the electron particle flux it detected only later, which roughly the same envelope as the ion particle flux (Fig. 2). This is because the parallel electric field acts to set up phase space eddies that maintain local quasineutrality. The electron power flux exceeds the ion power flux at the outer target. The total energy deposition is about the same for ions and electrons at the outer target due to the shorter duration of the electron pulse (Fig. 4). At the inner target the ion power flux exceeds the electron power flux. The ion pulse is observed after a delay $\Delta t_i \sim \mu^{1/2} \Delta t_e$, which is relatively insensitive to ELM Mach number (Fig. 3). The peak ion power flux is supposed to occur after a delay Δt_{IR} at roughly the same time as the target temperature measured by infrared cameras reaches its maximum value. The peak occurs slightly later at the outer target due to the lower mean velocity of ions. In experiment the outer target temperature peaks earlier. This is due to the fact the the ELM enters the SOL near the outboard midplane, so the transit time to the outer target is shorter than to the inner target. Presumably if we initiated the ELM close to the outer target rather than in the center of the domain, we would obtain similar results. The ratio of energy deposition to inner and outer targets is similar to that predicted by the simple ballistic ion model, but inclusion of the electron power becomes important as the ELM Mach number increases (Fig. 5).

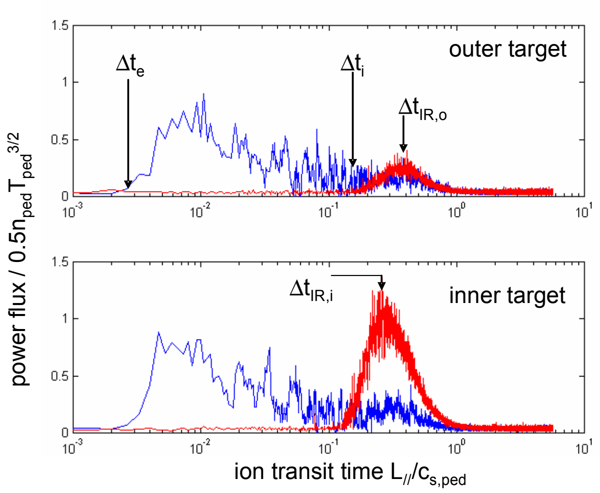

Fig. 1. Electron (blue) and ion (red) power flux to outer (upper panel) and inner (lower panel) divertor plates for M_{ELM}=0.35. The electron pulse is initially detected after a delay $\Delta t_e \sim L_{//}/2v_{Te,ped}$, and the ion pulse after $\Delta t_i \sim L_{//}/2v_{Ti,ped}$. The peak ion power flux occurs at times $\Delta t_{IR,o}$ and $\Delta t_{IR,i}$ at outer and inner targets, respectively. These times correspond to the peak IR temperatures in experiment.

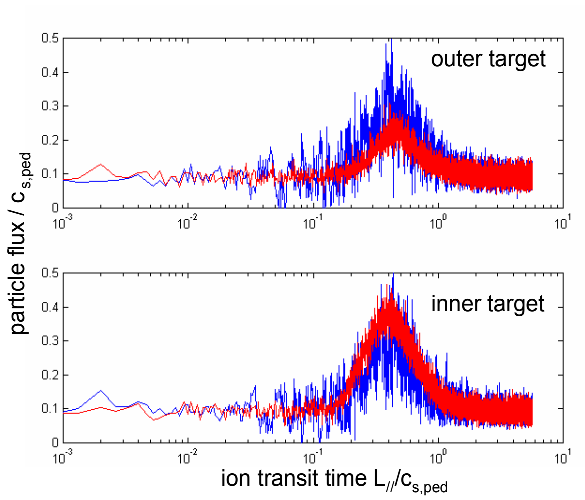

Fig. 2. Electron (blue) and ion (red) particle flux to outer (upper panel) and inner (lower panel) divertor plates.

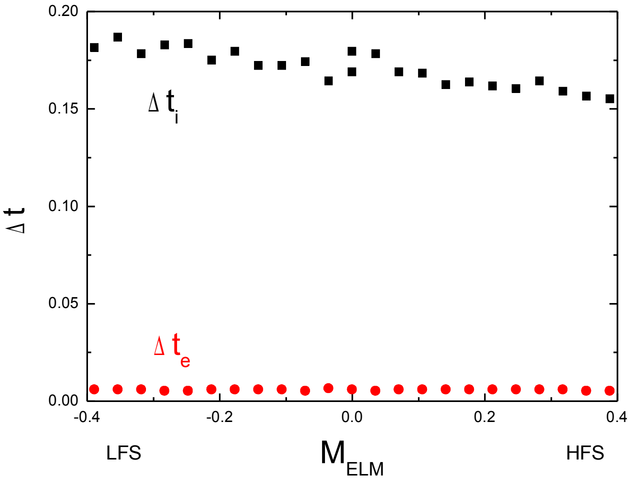

Fig. 3. Delay times, measured in hot ion transit times, for first detection of electron (red circles) and ion (black squares) heat pulses. Negative Mach number means outer divertor target, postive Mach number means inner divertor target.

Fig. 4. Total ion (black squares) and electron (red circles) energy deposited on each target plate vs. ELM Mach number (normalized to pedestal parameters). At the outer target (negative Mach numbers) the electron energy can exceed the ion energy.

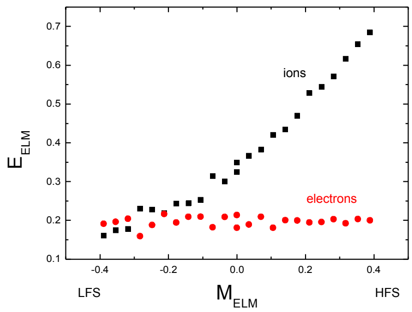

Fig. 5. Ratio of inner-to-outer target energy deposition. The ratios of total energy (black squares) and the ion energy alone (red circles) are shown.

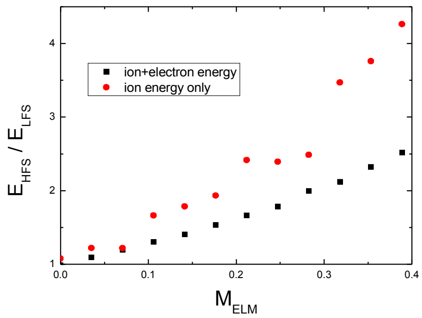

*Partly supported by the Czech Republic Grant Project GAČR 202/04/0360.

[1] A. Loarte, et al., Physics of Plasmas **11**, 2668 (2004).
[2] W. Fundamenski, et al., Plasma Phys. Control. Fusion **48**, 109 (2006).
[3] T. Eich, et al., 18th Conference on Plasma Surface Interactions, Toledo, May 2008, submitted to J. Nucl. Mater.
[4] D. Tskhakaya, et al., Contrib. Plasma Phys. **48**, 89 (2008).
[5] W. M. Manheimer, M. Lampe, G. Joyce, J. Comput. Phys. **138**, 563 (1997).
[6] J. P. Gunn, V. Fuchs, Phys. Plasmas **14**, 032501 (2007).
[7] K. -S. Chung, I. H. Hutchinson, Phys. Rev. A **38**, 4721 (1988).
[8] V. Fuchs, J. P. Gunn, Europ. Conf. Abstracts, **31F** P4-033 (2007).